

Ultra-Fast Reactive Transport Simulations When Chemical Reactions Meet Machine Learning: Chemical Equilibrium

Allan M. M. Leal^{a,*}
allan.leal@erdw.ethz.ch

Dmitrii A. Kulik^b
dmitrii.kulik@psi.ch

Martin O. Saar^a
msaar@ethz.ch

^a*Geothermal Energy and Geofluids Group,
Department of Earth Sciences, ETH Zürich, Switzerland*

^b*Laboratory for Waste Management, Nuclear Energy and Safety Research Department,
Paul Scherrer Institut, 5232 Villigen PSI, Switzerland*

Abstract

During reactive transport modeling, the computational cost associated with chemical reaction calculations is often 10–100 times higher than that of transport calculations. Most of these costs results from chemical equilibrium calculations that are performed at least once in every mesh cell and at every time step of the simulation. Calculating chemical equilibrium is an iterative process, where each iteration is in general so computationally expensive that even if every calculation converged in a single iteration, the resulting speedup would not be significant. Thus, rather than proposing a fast-converging numerical method for solving chemical equilibrium equations, we present a machine learning method that enables new equilibrium states to be quickly and accurately estimated, whenever a previous equilibrium calculation with similar input conditions has been performed. We demonstrate the use of this smart chemical equilibrium method in a reactive transport modeling example and show that, even at early simulation times, the majority of all equilibrium calculations are quickly predicted and, after some time steps, the machine-learning-accelerated chemical solver has been fully trained to rapidly perform all subsequent equilibrium calculations, resulting in speedups of almost two orders of magnitude. We remark that our new *on-demand machine learning method* can be applied to any case in which a massive number of sequential/parallel evaluations of a computationally expensive function f needs to be done, $y = f(x)$. We remark, that, in contrast to traditional machine learning algorithms, our on-demand training approach does not require a statistics-based training phase before the actual simulation of interest commences. The introduced on-demand training scheme requires, however, the first-order derivatives $\partial f/\partial x$ for later smart predictions.

1 Introduction

During reactive transport simulations, the following three degrees of chemical reactivity behavior may be observed across space and over time: weak, moderate, and intense. For example, at relatively distant locations from where a fluid enters a medium, none or little reactivity may occur, potentially over long periods of time, if those regions were initially in chemical, thermal, and

*Corresponding author

mechanical equilibrium. Eventually, these equilibrium conditions are gradually disrupted due to fluid flow, heat transfer, and chemical transport, causing some moderate chemical reactivity. Later, the introduced perturbations reach those once calm locations and cause relatively intense local chemical changes.

Interestingly, after such a wave of perturbations has passed, very often local chemical reactivity becomes weak once again. This implies that only a relatively small percentage of the entire medium is experiencing fast and substantial chemical changes at any moment in time. As a result, most chemical reaction calculations are performed for low-reactivity regions at every time step of the simulation. Even though reaction calculations are relatively faster in low-reactivity regions, compared to high-reactivity regions, their overall computational cost is typically 10–100 times greater than that for calculations of physical processes (e.g., mass transport, heat transfer). Thus, reactive transport simulations spend most of the computation time calculating chemical reactions and not transport processes, and typically require very long compute times. Hence, speeding up chemical calculations, without compromising accuracy, is crucial for significant performance gains in reactive transport simulations.

Whenever chemical reaction rates are considerably faster than rates of physical processes, the *local chemical equilibrium assumption* is a plausible and sufficient rate model for chemical reactions. In general, however, a combination of fast and slow reaction rates is present, so that the fast reactions are reasonably modeled employing the chemical equilibrium assumption and slow reaction rates are modeled using chemical kinetics. This approach is termed the *local partial chemical equilibrium assumption* [1–7]. Nevertheless, what needs to be noticed about these assumptions is that chemical equilibrium calculations are needed to model chemical processes in either case. In fact, such equilibrium calculations need to be performed at least once at every mesh node/cell during every transport time step. Thus, millions to billions of chemical equilibrium calculations tend to accumulate over the course of massive numerical reactive transport simulations, particularly when using fine-resolution meshes, large three-dimensional domains, and/or long simulation times. Hence, speeding up reactive transport modeling by a significant factor can only be accomplished by *accelerating chemical reaction calculations in general, and chemical equilibrium calculations in particular*. Here, we focus on accelerating chemical equilibrium calculations, whereas a companion paper (Leal et al. [8]) introduces a similar strategy to accelerate chemical kinetics calculations.

Chemical equilibrium calculations are computationally expensive. This is because (i) they involve the iterative solution of a system of non-linear algebraic equations, requiring at every iteration (ii) the evaluation of thermodynamic properties, such as activity coefficients, concentrations, activities, chemical potentials (e.g., using the Pitzer [9] model for aqueous solutions and the Peng and Robinson [10] model for gaseous solutions), and (iii) the solution of a system of linear equations with dimension on the order of either the number of chemical species or the number of chemical elements [11]. Over several decades, major advances in developing fast, accurate, and robust methods for chemical equilibrium calculations have been made, either based on *Gibbs energy minimization* (GEM) or *law of mass action* (LMA) formulations [11–41]. However, even if one could devise an algorithm that would always converge in one single iteration, instead of the typical few to dozens of iterations, the computational cost of chemical equilibrium calculations would still be dominant among all other calculations. The question of utmost importance is, thus: *Is it possible to calculate chemical equilibrium without actually solving the non-linear equations governing equilibrium, which requires several evaluations of thermodynamic models and as many solutions of systems of linear equations?* In this paper, we demonstrate that this can, indeed, be achieved with exceptional speed and accuracy.

Our here-introduced smart chemical equilibrium algorithm operates like a human being. A human begins life with none to little problem solving skills. At an early age, the child is exposed to a variety of challenges and learns how to solve them, often with assistance from others. However, once the child has learned how to solve a specific problem, it can solve *similar problems* without requiring assistance. Solving a problem with the help of an already acquired skill is *much faster* than having to first learn how to solve that problem, since *learning* is a difficult and time-consuming process. As the child grows, it can solve more and more problems until, eventually, as an adult, external help is needed only occasionally, under exceptional circumstances, i.e., in situations that have rarely or never been encountered before. Importantly, in contrast to going to school, this way of “learning by doing” may be viewed as on-demand learning or training, a highly efficient way of learning as one only learns what is actually needed at least once.

The above metaphor illustrates some key features of our new, on-demand machine learning algorithm for fast chemical equilibrium calculations. Initially, the algorithm has no recollection of any past calculation. Thus, the first time the algorithm faces a new chemical equilibrium problem, it fully solves the problem and saves the inputs and outputs describing the calculated equilibrium state. This is, as discussed previously, a computationally expensive process, now considered as an act of learning. The next time the algorithm is employed, it recalls that a calculation has previously been performed and attempts to quickly predict the new chemical equilibrium state, using *sensitivity derivatives* to project the previously recorded equilibrium state into the new one. Then, the algorithm checks if the prediction is accurately acceptable within some given tolerance. If it is, then the predicted equilibrium state is accepted as a solution, otherwise a full chemical equilibrium calculation is performed and the corresponding inputs and outputs recorded to describe the newly learned equilibrium state. This way, the memory of past and fully solved equilibrium problems grows, permitting searches among all saved and learned problems to determine the one that is closest to the new equilibrium problem.

In contrast to traditional machine learning algorithms, which first require a time-consuming training phase, in which potentially many outcomes are calculated for problems that may later never occur, our new machine learning algorithm is only trained with problems that actually occur, relying on the recurrence of subsequent *similar problems* to quickly respond with an accurate prediction. Hence, traditional machine learning is equivalent to going to school, while our machine learning algorithm is more akin to on-demand learning or “learning by doing.” Furthermore, there is no clear criterion to decide, when the training phase of traditional machine learning algorithms is ideally terminated, i.e., when it is time to “leave school.”

The here-introduced smart chemical equilibrium algorithm is particularly useful for applications that require repetitive calculations, such as chemical equilibrium calculations during reactive transport modeling. For such applications, the algorithm can eventually achieve a knowledgeable state, so that, after some time steps during a reactive transport simulation, all equilibrium calculations can be rapidly and accurately performed using previously learned *key chemical equilibrium states*. Even if the smart algorithm occasionally faces some exceptional circumstances that require additional on-demand training (e.g., a sudden change in the chemistry or temperature of the fluid entering a region of the medium), one can still reasonably expect significant speedups with this machine-learning-accelerated algorithm, if the occasions during which learning is needed are considerably less frequent than the occasions during which the algorithm can make smart predictions.

The “intelligence” of the here-introduced algorithm is, thus, a combination of both the memory of already solved equilibrium problems, that needed to be solved anyway, and its ability to “learn” new ones on-demand. Physiologically speaking, the algorithm is like a *brain* that not only can

record its experiences on solving chemical equilibrium problems, but can also make decisions about when it needs additional training, following its judgment on the accuracy/acceptability of an estimated chemical equilibrium outcome. This on-demand training is key to:

- (i) *Performance*: learning and keeping only what is needed results in compact storage and thus fast search operations when finding the closest past equilibrium problem already solved;
- (ii) *Accuracy*: finer control on minimizing errors resulting from predicted equilibrium states by performing additional training whenever needed;
- (iii) *Convenience*: neither a dedicated prior training stage nor anticipation of possible chemical conditions during the simulation are required;
- (iv) *Simplicity*: users immediately benefit from high-performance reactive transport simulations without having to prepare any prior configuration and training of the smart chemical equilibrium solver.

Our on-demand training philosophy differs radically from most previous efforts in speeding up chemical reaction calculations in reactive transport simulations, which use conventional machine learning methods. Jatnieks et al. [42], for example, present the steps necessary to construct a so-called surrogate model for fast speciation calculations. The construction of this surrogate model requires a prior training phase, during which many random input conditions are used in a speciation solver (PHREEQC [43]) and the resultant outputs collected for statistical learning. During their numerical experiment, 32 different statistics and machine learning methods were tried to identify the potentially best one. For a specific reactive transport modeling problem, they collected all possible input-output combinations in speciation calculations, and from these combinations, 7880 random inputs were used for training the statistics model, which represented 80% of all collected input conditions. The various constructed surrogate models were subsequently used in a reactive transport simulation. Each surrogate model was constructed with different 7880 input-output samples.

Our new *on-demand machine learning approach* has clear advantages over conventional statistics-based machine learning methods. First, the use of sensitivity derivatives of the calculated equilibrium states results in a machine learning method that better understands the behavior of chemical systems regarding its reaction behavior following changes in the input equilibrium conditions. Secondly, the use of these sensitivity derivatives permits extrapolating and predicting new equilibrium states with much higher accuracy and confidence. Thirdly, it requires no statistical training before it can be applied in a reactive transport simulation, because its on-demand training characteristics allow it to spontaneously learn only what is needed during a reactive transport simulation to keep the predictions accurate enough. Furthermore, our approach is not only simpler from a user point of view, but also potentially faster, as it will save only a few input conditions compared to any statistical approach that can only get more accurate the more it knows a priori. Finally, our method produces outputs that always satisfy the mass conservation conditions of chemical elements and electric charge, since these constraints are incorporated into the calculation of the sensitivity derivatives (see Leal et al. [11]) and, thus, our method contrasts with statistics-based machine learning methods that can fail predicting equilibrium states that satisfy given mass balance conditions.

This communication is organized as follows. In Section 2, we introduce definitions and notation that are needed to describe the new algorithm rigorously. In Section 3, we formulate the smart chemical equilibrium method, providing details on the prediction of new equilibrium states from

previously saved and learned states as well as on the acceptance criteria for the predicted equilibrium states. In Section 4, we compare the performance and accuracy of a reactive transport simulation using the here-proposed smart equilibrium algorithm against that using a conventional Newton-based equilibrium algorithm. Finally, we discuss in Section 5 the implications and conclusions of this study together with a planned road-map for further research efforts in this direction.

The here-introduced smart chemical equilibrium algorithm is implemented in Reaktoro [?], a unified open-source framework for modeling chemically reactive systems (reaktoro.org).

2 Definitions and Notation

Consider a chemical system is a collection of *chemical species* composed of one or more *components* and distributed among one or more *phases*. The species can be substances such as aqueous ions (e.g., $\text{Na}^+(\text{aq})$, $\text{Cl}^-(\text{aq})$, $\text{HCO}_3^-(\text{aq})$), neutral aqueous species (e.g., $\text{SiO}_2(\text{aq})$, $\text{CO}_2(\text{aq})$, $\text{H}_2\text{O}(\text{l})$), gases (e.g., $\text{CO}_2(\text{g})$, $\text{CH}_4(\text{g})$, $\text{N}_2(\text{g})$), and pure condensed phases (e.g., $\text{CaCO}_3(\text{s, calcite})$, $\text{SiO}_2(\text{s, quartz})$, $\text{Al}_2\text{Si}_2\text{O}_5(\text{OH})_4(\text{s, kaolinite})$). The phases are each composed of one or more different chemical species with homogeneous properties within their boundaries; a phase can be aqueous, gaseous, liquid, solid solutions, a pure mineral, a plasma, etc. Note that substances with the same chemical formula, but in different phases, are distinct species (e.g., $\text{CO}_2(\text{aq})$ and $\text{CO}_2(\text{g})$ are different species). The components are *chemical elements* (e.g., H, O, C, Na, Cl, Ca, Si) and *electrical charge (Z)*, but it can also be a linear combination of these, commonly known as *primary species* (e.g., $\text{H}^+(\text{aq})$, $\text{H}_2\text{O}(\text{l})$, $\text{CO}_2(\text{aq})$). We shall use from now on the words elements and components interchangeably, with elements not only denoting chemical elements but also electrical charge [11].

A chemical system can exist at infinitely many *chemical states*. A chemical state is defined here as the triplet (T, P, n) , where T is temperature, P is pressure, and $n = (n_1, \dots, n_N)$ is the vector of molar amounts of the species, with n_i denoting the mole amount of the i th species and N the number of species. If we denote by $b = (b_1, \dots, b_E)$ the vector of molar amounts of the elements, with b_j denoting the amount of the j th element and E the number of elements, then b and n are related through the following mass conservation equation:

$$An = b, \quad (1)$$

where A is the *formula matrix* of the chemical system [14], with A_{ji} denoting the coefficient of the j th element in the i th species, and thus a matrix with dimensions $E \times N$. Below is an example of a formula matrix for a simple chemical system, containing $N = 10$ species and $E = 4$ elements, distributed among two phases, namely an aqueous and a gaseous phase, with names of aqueous species suffixed with (aq), except $\text{H}_2\text{O}(\text{l})$, and gaseous species with (g):

$$A = \begin{matrix} & \text{H}_2\text{O}(\text{l}) & \text{H}^+(\text{aq}) & \text{OH}^-(\text{aq}) & \text{CO}_2(\text{aq}) & \text{HCO}_3^-(\text{aq}) & \text{CO}_3^{2-}(\text{aq}) & \text{O}_2(\text{aq}) & \text{H}_2(\text{aq}) & \text{CO}_2(\text{g}) & \text{H}_2\text{O}(\text{g}) \\ \text{H} & \left[\begin{array}{cccccccccc} 2 & 1 & 1 & 0 & 1 & 0 & 0 & 2 & 0 & 2 \\ 1 & 0 & 1 & 2 & 3 & 3 & 2 & 0 & 2 & 1 \\ 0 & 0 & 0 & 1 & 1 & 1 & 0 & 0 & 1 & 0 \\ 0 & 1 & -1 & 0 & -1 & -2 & 0 & 0 & 0 & 0 \end{array} \right. & \end{matrix} \quad (2)$$

In the mathematical presentation that follows, we assume, for convenience reasons, that the formula matrix A , of the corresponding chemical system, is full-rank (i.e., the rows of A are linearly independent) so that $\text{rank}(A) = E$.

3 Method

Let a chemical equilibrium calculation be represented as:

$$n = \varphi(T, P, b). \quad (3)$$

The chemical equilibrium function, φ , is an abstraction of the operations needed to solve the fundamental Gibbs energy minimization problem:

$$\min_n G(T, P, n) \quad \text{subject to} \quad \begin{cases} An = b \\ n \geq 0 \end{cases}, \quad (4)$$

at prescribed conditions of temperature, T , pressure, P , and element amounts, $b = (b_1, \dots, b_E)$. In this problem, one seeks $n = (n_1, \dots, n_N)$ that minimizes the total Gibbs energy function of the system:

$$G = \sum_{i=1}^N \mu_i n_i, \quad (5)$$

subject to the elemental mass conservation constraint equations, $An = b$, and the non-negativity constraints for the species amounts, $n_i \geq 0$. The *chemical potential* of the i th species, $\mu_i = \mu_i(T, P, n)$, is defined as:

$$\mu_i = \mu_i^\circ + RT \ln \alpha_i, \quad (6)$$

with R denoting the universal gas constant, $\mu_i^\circ = \mu_i^\circ(T, P)$ the *standard chemical potential* of the i th species, and $\alpha_i = \alpha_i(T, P, n)$ the *activity* of the i th species. More details on how this chemical equilibrium problem can be solved, using either Gibbs energy minimization (GEM) or law of mass action (LMA) methods, are presented in Section A or in more detail in Leal et al. [11, 32, 33].

3.1 First-Order Taylor Approximation

Assume a chemical equilibrium calculation has been done previously with inputs (T^p, P^p, b^p) , and the new chemical equilibrium calculation needs to be performed with inputs (T^q, P^q, b^q) . Rather than computing n^q using the computationally expensive chemical equilibrium function φ :

$$n^q = \varphi(T^q, P^q, b^q), \quad (7)$$

we want to try first to estimate n^q using the following *first-order Taylor approximation*:

$$n^q = n^p + \frac{\partial \varphi^p}{\partial T} (T^q - T^p) + \frac{\partial \varphi^p}{\partial P} (P^q - P^p) + \frac{\partial \varphi^p}{\partial b} (b^q - b^p), \quad (8)$$

where $\partial \varphi^p / \partial T$, $\partial \varphi^p / \partial P$, and $\partial \varphi^p / \partial b$ are *sensitivity derivatives* (with dimensions $N \times 1$, $N \times 1$, and $N \times E$, respectively) of the previous chemical equilibrium state. These sensitivity derivatives are measures of how the species amounts change when the previous chemical equilibrium state is perturbed by infinitesimal changes in temperature, pressure, and the amounts of elements. They can be equivalently written as $\partial n^p / \partial T$, $\partial n^p / \partial P$, and $\partial n^p / \partial b$.

By using these sensitivity derivatives, we can quickly and accurately estimate all chemical equilibrium states in the vicinity of some previous, and fully known, chemical equilibrium state.

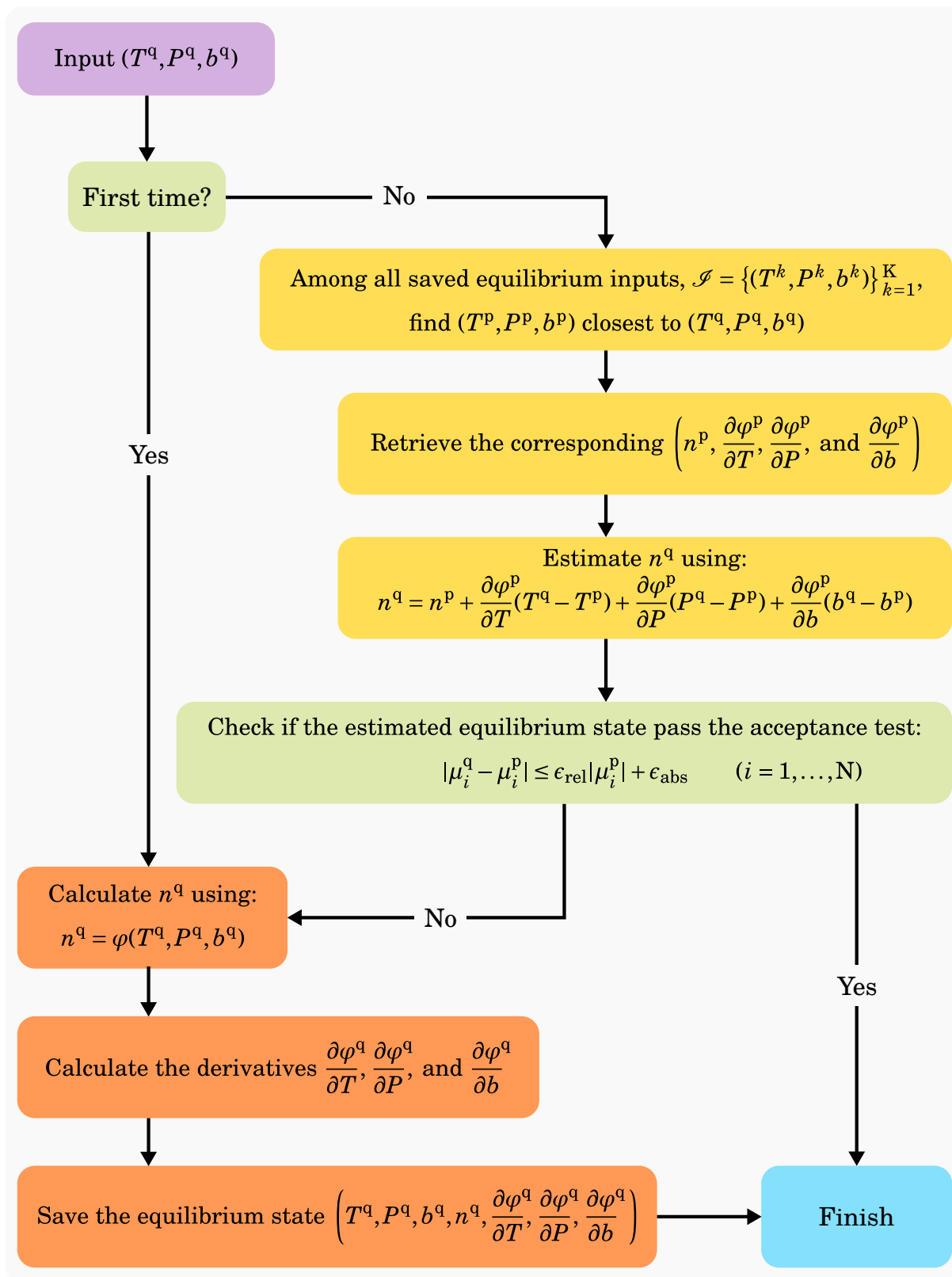


Figure 1: The diagram of the proposed machine learning algorithm for fast chemical equilibrium calculations with a supervised, on-demand training strategy.

3.2 Acceptance Testing

Once a predicted chemical equilibrium state is calculated, one needs to test if it can be accepted. Because we are using a first-order Taylor approximation, we need to ensure that the new estimated chemical equilibrium state is not too far from the previous fully-calculated equilibrium state, used as a reference point. This could be done naively by checking how much the species amounts changed from one state to the other using the following test condition for all species:

$$|n_i^q - n_i^p| \leq \epsilon_{\text{rel}} |n_i^p| + \epsilon_{\text{abs}} \quad (i = 1, \dots, N), \quad (9)$$

which controls how much the absolute and relative changes in the new estimated species amounts, n_i^q , can be tolerated for given absolute and relative tolerance parameters ϵ_{abs} and ϵ_{rel} , respectively.

However, there is a major disadvantage of the previous tolerance test: it does not “understand” the *thermodynamic behavior of stable phases*. Consider a chemical system with two stable phases: an aqueous solution saturated with a mineral. Clearly, adding more of that mineral to the system will not alter the composition of the fluid and just accumulate to a higher total amount of solids. Under such conditions, the acceptance test based on species amounts would fail, even though the estimated chemical equilibrium state, using sensitivity derivatives, could be done very accurately for *any large amounts* of added mineral. By adding 1000 moles of the mineral, and enforcing the constraint that, for example, not more than 10% of a species amount can vary from the previous state to the new estimated state, that acceptance test would trigger hundreds of unnecessary training equilibrium calculations if the initial mineral amount is 1 mol.

For the previous example, assuming the perturbation of the system is made only by adding the mineral, i.e., without changing temperature or pressure, there is one thermodynamic quantity that would remain constant: the *chemical potentials of the species*, μ_i . Because of this behavior, we use instead the following acceptance test in terms of chemical potentials:

$$|\mu_i^q - \mu_i^p| \leq \epsilon_{\text{rel}} |\mu_i^p| + \epsilon_{\text{abs}} \quad (i = 1, \dots, N), \quad (10)$$

where μ_i^q is the estimated, *not evaluated*, chemical potential of the i th species at the new chemical equilibrium state:

$$\mu^q = \mu^p + \frac{\partial \mu^p}{\partial T} (T^q - T^p) + \frac{\partial \mu^p}{\partial P} (P^q - P^p) + \frac{\partial \mu^p}{\partial n} (n^q - n^p), \quad (11)$$

where $\partial \mu^p / \partial T$, $\partial \mu^p / \partial P$, and $\partial \mu^p / \partial n$ are chemical potential derivatives (with dimensions $N \times 1$, $N \times 1$, and $N \times N$, respectively) evaluated at the previous equilibrium state.

Remark: For LMA methods, in which no access to standard chemical potentials, μ_i° , exists in some cases (e.g., the thermodynamic database used only contains equilibrium constants of reactions), a similar, but *not equivalent*, test is the use of activities:

$$|\ln a_i^q - \ln a_i^p| \leq \epsilon_{\text{rel}} |\ln a_i^p| + \epsilon_{\text{abs}} \quad (i = 1, \dots, N). \quad (12)$$

Note, however, that activities are in general less sensitive to temperature variations than standard chemical potentials and, thus, the above alternative acceptance test would be less rigorous than equation (10) and more indifferent towards temperature changes. To fix this problem, one could use the conversion approach detailed in Leal et al. [44], which permits apparent standard chemical potentials of the species to be calculated using equilibrium constants of reactions.

3.3 Machine Learning Chemical Equilibrium Algorithm

The machine learning chemical equilibrium algorithm (or, alternatively, smart chemical equilibrium algorithm) proposed here is capable of “remembering” past calculations and can make use of these calculations to quickly and accurately estimate new equilibrium states. Figure 1 is a flowchart that illustrates the main steps of the algorithm.

During its first chemical equilibrium calculation, with given (T^q, P^q, b^q) conditions, the algorithm does so by solving the Gibbs energy minimization problem (4). This is represented here, using the computationally expensive equilibrium function, φ :

$$n^q = \varphi(T^q, P^q, b^q). \quad (13)$$

Once this is done, we need to save not only the input conditions (T^q, P^q, b^q) , but also the corresponding, calculated equilibrium amounts of species, n^q ; the sensitivity derivatives of this equilibrium state, $\partial\varphi^q/\partial T$, $\partial\varphi^q/\partial P$, and $\partial\varphi^q/\partial b$, needed by equation (8); and the derivatives of the chemical potentials, $\partial\mu^q/\partial T$, $\partial\mu^q/\partial P$, and $\partial\mu^q/\partial n$, needed by equation (11). See Leal et al. [11] for a description of how to calculate these derivatives. By saving these state values, we will later be able to make fast and accurate predictions of all equilibrium states in the vicinity of the one just recorded.

The next time the algorithm is asked to solve a new equilibrium problem, it does so by first searching, among all saved equilibrium input conditions:

$$\mathcal{S} = \{(T^k, P^k, b^k)\}_{k=1}^K, \quad (14)$$

the input (T^p, P^p, b^p) that is closest to the given one (T^q, P^q, b^q) , where “closest” is measured here in the sense of the Euclidean norm (other norms can be implemented as well):

$$d^k = \left[(T^q - T^k)^2 + (P^q - P^k)^2 + \sum_{j=1}^E (b_j^q - b_j^k)^2 \right]^{\frac{1}{2}}, \quad (15)$$

where d^k is a scalar that measures the difference between (T^q, P^q, b^q) and (T^k, P^k, b^k) . Once the search is concluded, the previously calculated equilibrium state, corresponding to input conditions (T^p, P^p, b^p) , can be used to estimate the equilibrium state corresponding to input conditions (T^q, P^q, b^q) using equation (8).

Finally, it remains to check if the estimated equilibrium state is potentially accurate enough using the acceptance test defined by equation (10). If the test succeeds, then the equilibrium calculation ends. Otherwise, a complete chemical equilibrium calculation at (T^q, P^q, b^q) conditions is performed, $n^q = \varphi(T^q, P^q, b^q)$, and the corresponding sensitivity derivatives of the fully computed equilibrium state ($\partial\varphi^q/\partial T$, $\partial\varphi^q/\partial P$, and $\partial\varphi^q/\partial b$) are evaluated, which are then finally saved for possible future use when estimating equilibrium states under (T, P, b) conditions in the vicinity of the just recorded (T^q, P^q, b^q) conditions.

4 Results

We now present the use of the machine learning method for smart chemical equilibrium calculations in a reactive transport simulation and show how its performance compares with the use of a

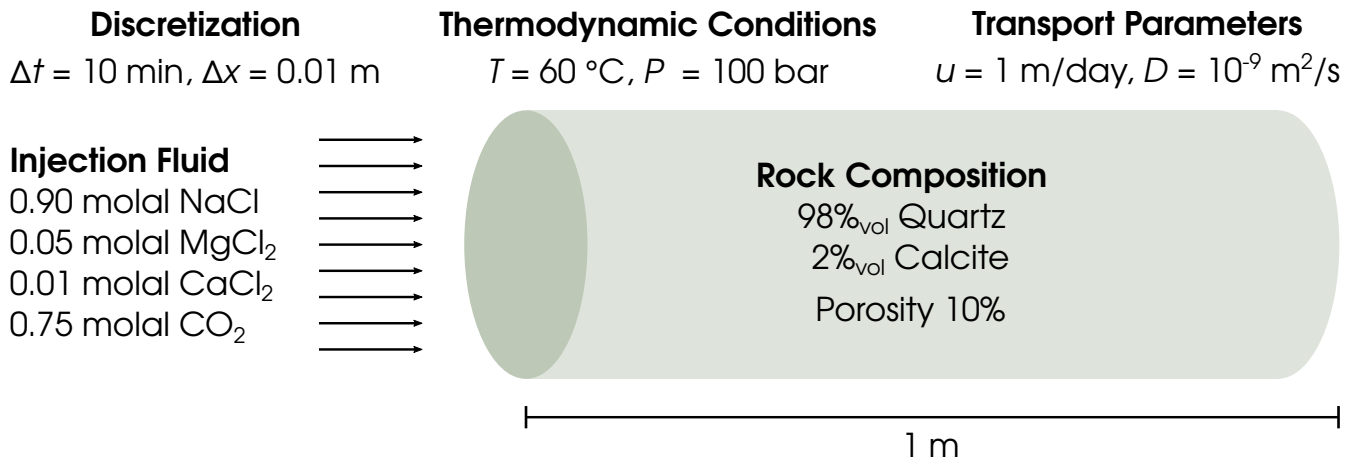


Figure 2: Illustration of the reactive transport modeling along a rock core, with details of the injection fluid and rock composition, transport parameters, and numerical discretization.

conventional chemical equilibrium algorithm. For details on how we solve the reactive transport equations, see Appendix B.

Figure 2 illustrates the reactive transport modeling carried out in this work to investigate the efficiency of the proposed smart chemical equilibrium calculations for sequential calculations. It shows the injection of an aqueous fluid resulting from the mixture of 1 kg of water with 0.90 moles of NaCl, 0.05 moles of MgCl₂, 0.01 moles of CaCl₂, and 0.75 moles of CO₂, in a state very close to CO₂ saturation, and thus in an acidic state with a calculated pH of 4.65. The initial rock composition is 98%_{vol} SiO₂(quartz) and 2%_{vol} CaCO₃(calcite), with an initial porosity of 10%. The resident fluid is a 0.70 molal NaCl brine in equilibrium with the rock minerals, with a calculated pH of 10.0. The temperature and pressure of the fluids are 60 °C and 100 bar, respectively. The reactive transport modeling procedure assumes a constant fluid velocity of $v = 1 \text{ m/day}$ ($1.16 \cdot 10^{-5} \text{ m/s}$) and the same diffusion coefficient $D = 10^{-9} \text{ m}^2/\text{s}$ for all fluid species, without dispersivity.

The activity coefficients of the aqueous species are calculated using the HKF extended Debye-Hückel model [45–48] for solvent water and ionic species, except for the aqueous species CO₂(aq), for which the Drummond [49] model is used. The standard chemical potentials of the species are calculated using the equations of state of Helgeson and Kirkham [45], Helgeson et al. [50], Tanger and Helgeson [51], Shock and Helgeson [52] and Shock et al. [53]. The database file `slop98.dat` from the software SUPCRT92 [54] is used to obtain the parameters for the equations of state. The equation of state of Wagner and Pruss [55] is used to calculate the density of water and its temperature and pressure derivatives. Kinetics of dissolution and precipitation of both calcite and dolomite is neglected in this particular example (i.e., the local equilibrium assumption is employed).

Figure 3 shows the volumes of the minerals calcite, CaCO₃, and dolomite, CaMg(CO₃)₂, as well as the concentrations of aqueous species Ca²⁺(aq), Mg²⁺(aq), HCO₃⁻(aq), CO₂(aq), and H⁺(aq) along the rock core at three different simulation times: 10 minutes, 1 hour, and 20 hours. As calcite dissolves, Ca²⁺(aq) ions are released into the aqueous solution, which react with the incoming Mg²⁺(aq) ions from the left boundary to precipitate dolomite. After 10 minutes of injecting the CO₂-saturated brine, one observes a slight dissolution of calcite and a corresponding precipitation of dolomite. The injected CO₂-saturated brine increases the local concentrations of carbonic species, CO₂(aq) and HCO₃⁻(aq). The local concentration of ions Ca²⁺(aq) also increase as a result of CaCO₃ dissolution. The precipitated dolomite, however, is gradually dissolved, as the injection

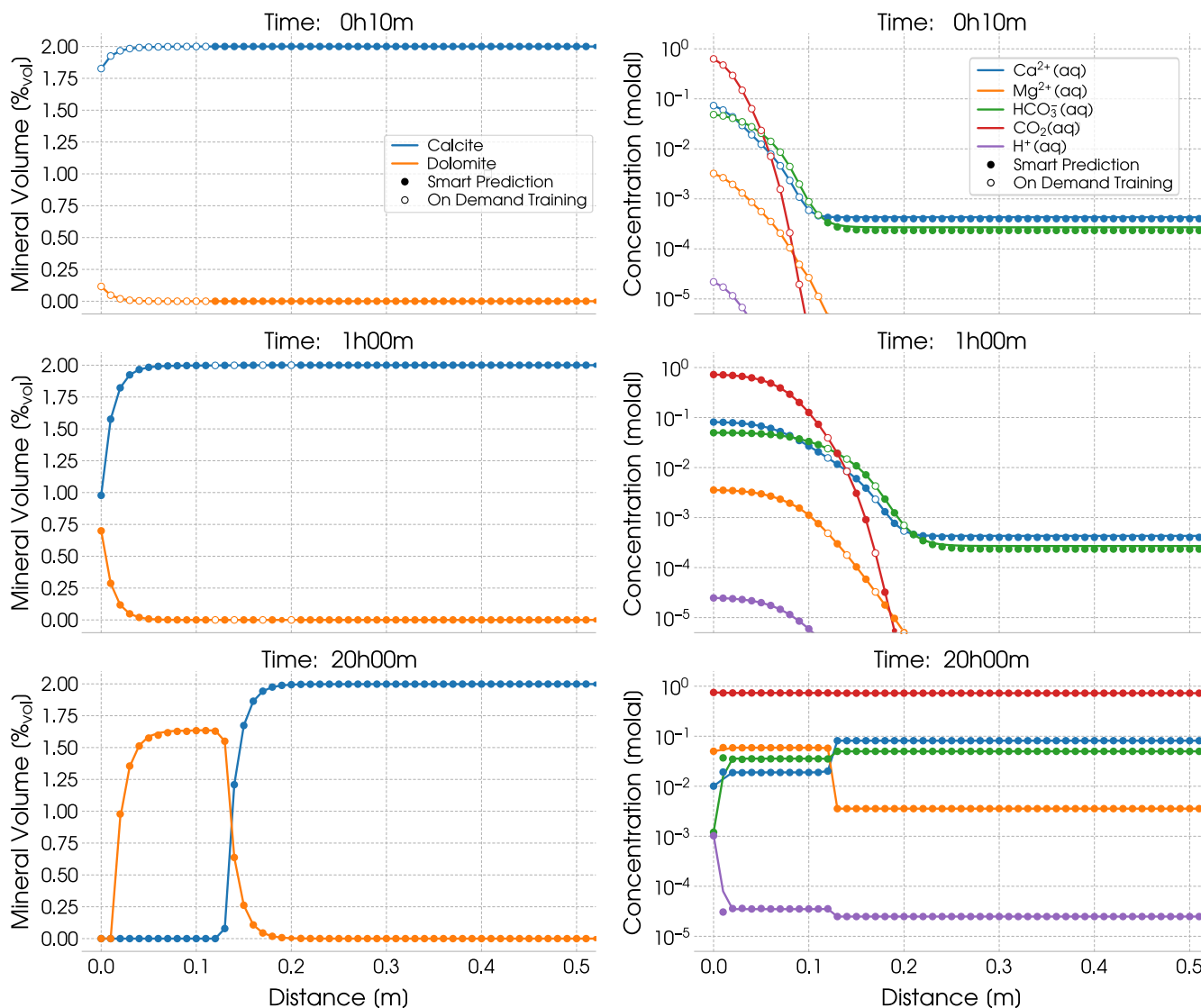


Figure 3: The volume of minerals calcite and dolomite (in %_{vol}) and the concentrations of selected aqueous species (in molal) along the rock core at three different times: 10 minutes, 1 hour, and 20 hours. The *solid curves* correspond to solving the reactive transport equations using expensive full chemical equilibrium calculations (reference curves). The *filled circles* (•) denote occasions in which equilibrium states are smartly predicted using previously recorded equilibrium states by the machine learning algorithm, and the *empty circles* (◦) denote occasions in which *on-demand training* is needed by the machine learning algorithm to learn a new chemical equilibrium state.

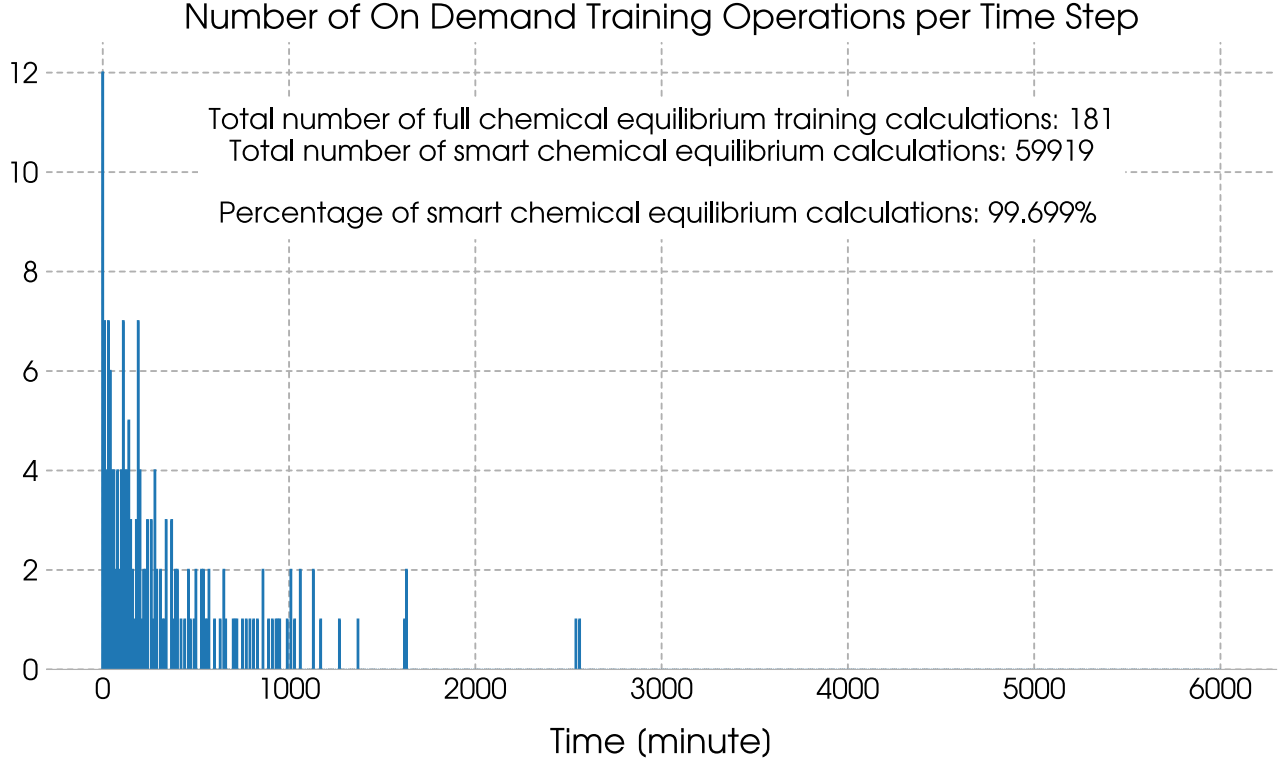


Figure 4: The recorded number of *on-demand training* occasions needed by the machine learning algorithm for smart chemical equilibrium calculations during each time step (10 minutes) of the reactive transport simulation (finished after 600 time steps, totaling 6000 minutes of simulation). Each training required the full solution of the non-linear equations governing chemical equilibrium using a Newton-based numerical method [32], which we show here to be considerably more computationally expensive than both transport calculations and the cost of smart equilibrium calculations accelerated with our machine learning strategy.

of the acidic CO_2 -saturated fluid continues. This can be seen in Figure 3, in the left region of the rock core, where neither calcite nor dolomite are present after 20 hours of continuous fluid injection. Also after 20 hours of fluid injection, the $\text{Mg}^{2+}(\text{aq})$ concentration drops sharply between core distances 0.1 m and 0.2 m, which is exactly where dolomite is currently precipitating.

Common to all sub-figures in Figure 3 is the use of *solid curves* to denote the reactive transport results using conventional, and thus computationally expensive, chemical equilibrium calculations throughout the simulation. These curves are used as a reference case for the results obtained using the here-proposed *machine learning algorithm for smart chemical equilibrium calculations* applied to the same reactive transport problem (see Section 3.3). Both the *filled circles* (\bullet) and the *empty circles* (\circ) are used to mark the calculated mineral volumes and species concentrations in Figures 3 using the smart equilibrium algorithm accelerated with machine learning. However, while the filled circles (\bullet) represent occasions, where the machine learning algorithm was able to quickly and successfully predict an accurate equilibrium state, the empty circles (\circ) represent occasions in which the smart algorithm required on-demand training to learn a new chemical equilibrium problem. These on-demand learning occasions happen at different mesh cells, either at the same time step or at different ones. The on-demand training operation is

needed, since the machine learning algorithm is faced with an equilibrium problem for which no accurate-enough prediction can be made. We remark that our proposed machine learning algorithm, for smart chemical equilibrium calculations, does not need to know any spatial or temporal information, although this could be explored for faster search operations in the future.

The machine learning algorithm starts without any recollection of previous chemical equilibrium calculations. It is initially trained during two occasions: when calculating the *initial equilibrium state* between the resident fluid and the rock minerals and when calculating the *equilibrium state of the injected fluid* at the left boundary. We can see in Figure 3 that during the first time step of the simulation, from time 0 to 10 minutes, the smart equilibrium algorithm was able to accurately estimate the equilibrium states in most mesh cells (see the filled circles •). All these successful quick estimates were done using *only one out of the two initial saved equilibrium states*: the initial equilibrium state of fluid species and rock minerals.

As the reactive fluid is injected inside the rock core, this promotes strong compositional changes in both resident fluid and rock minerals. Because of this, we can see that the machine learning algorithm required during the first time step, at 10 minutes, *on-demand training* in the first 12 cells (see the empty circles ◦). As the perturbation fronts move down the rock core, additional training is performed as needed to fulfill a given accuracy criterion (using $\epsilon_{\text{rel}} = \epsilon_{\text{abs}} = 0.1$). As seen in Figure 3, at 1h, or after 6 time steps, where strong concentration changes are occurring between 0.1 m and 0.2 m, there were 4 mesh cells that required full and expensive chemical equilibrium calculations for both accuracy and on-demand learning purposes. Eventually, the smart equilibrium algorithm gains enough knowledge about the recurring equilibrium states during the simulation, so that it is then able to quickly and accurately perform all equilibrium calculations without further training, as seen after 20h of fluid injection, or after 120 time steps (when only filled circles • are present).

Figure 4 shows how many on-demand training occasions were needed at each time step. During each of these training operations, a full chemical equilibrium calculation, using a conventional Newton-based algorithm, as presented in Leal et al. [32], is performed and the sensitivity derivatives of the equilibrium state are calculated for learning reasons. Figure 4 shows some relatively intense learning activities during the first 1000 minutes of simulated time (or 100 time steps) as expected, since the machine learning algorithm is constantly facing new equilibrium challenges in the beginning of its life. During the first time step, 12 on-demand training operations are needed, exactly in the first 12 mesh cells, in a mesh containing 100 cells (see empty circles ◦ in Figure 4 at 10 minutes). This implies that during the first time step, the machine learning algorithm was not yet trained enough to accurately predict the equilibrium states in those cells. During the second time step, 7 additional on-demand training operations are carried out and, as the simulation continues, only 1–2 additional training cases happen subsequently per time step, until the smart chemical equilibrium algorithm no longer requires any further learning (after about 258 time steps of 10 minutes of simulated time each). At this point, the machine learning algorithm is able to quickly and accurately predict all subsequent equilibrium states in every mesh cell, at every time step. For the reactive transport modeling problem chosen here, from the total of 60,000 equilibrium calculations needed, only 181 of these were actually performed using the expensive Newton-based chemical equilibrium algorithm, so that 99.7% of all such calculations were quickly performed using the proposed machine learning algorithm for fast chemical equilibrium calculations.

Figure 5 compares the computational cost per time step for conventional and smart chemical equilibrium calculations with the cost for transport calculations. The computational costs are measured in CPU time (in seconds). For the equilibrium calculations, it is the CPU time taken

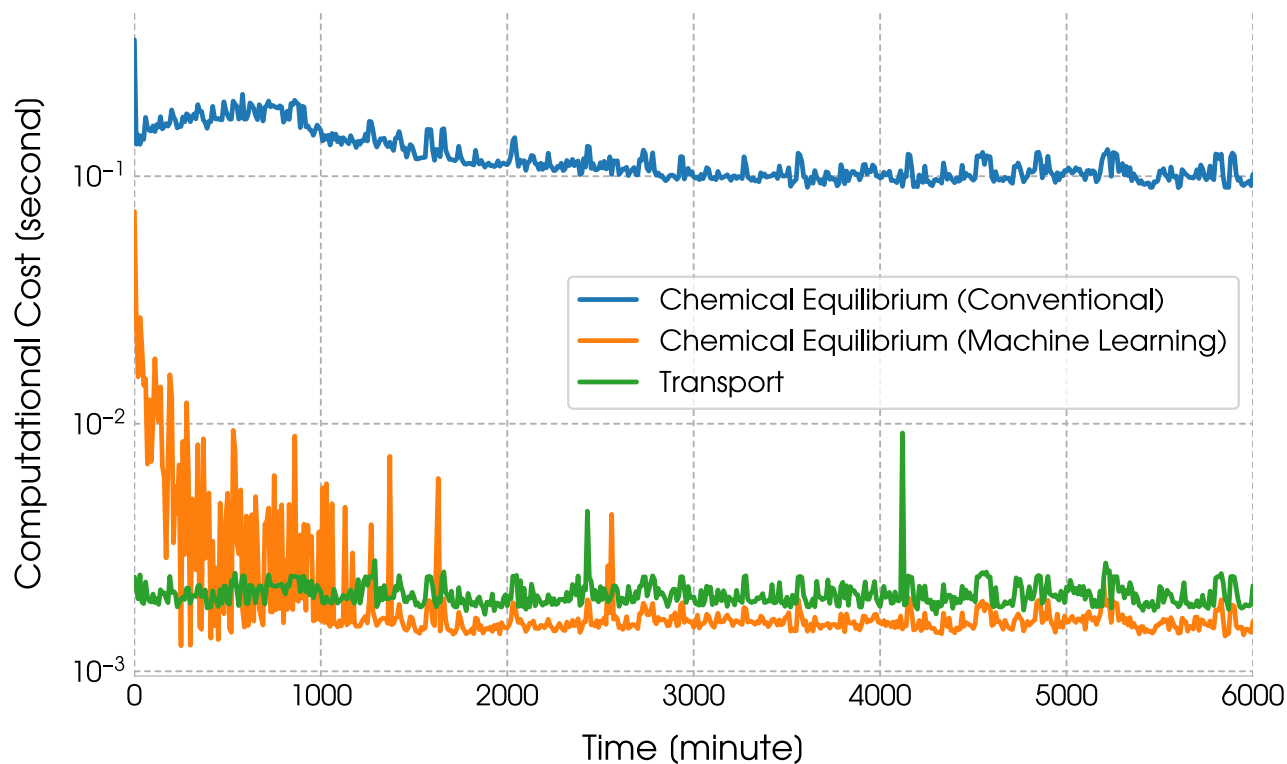


Figure 5: The comparison of the computational cost of transport, conventional chemical equilibrium, and machine-learning-accelerated chemical equilibrium calculations in each time step of the reactive transport simulation. The computational cost is given as CPU time (in seconds). The cost of equilibrium calculations per time step is the sum of the individual cost in each mesh cell. The cost of transport calculations per time step is the cost of solving the discretized algebraic transport equations. Our proposed machine learning strategy, based on predictions using sensitivity derivatives, can significantly speedup chemical equilibrium calculations by almost two orders of magnitude in this specific example.

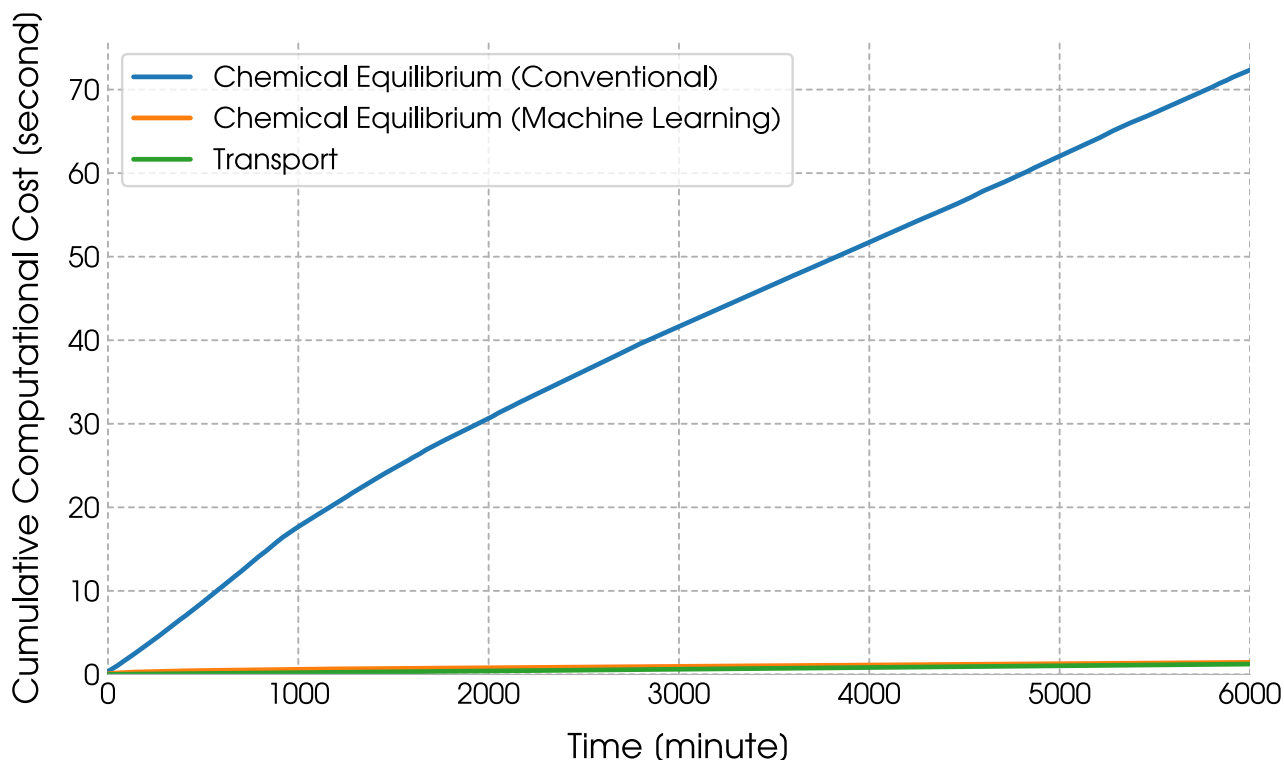


Figure 6: The cumulative computational cost of transport, conventional chemical equilibrium, and machine-learning-accelerated chemical equilibrium calculations as the reactive transport simulation continues. Our proposed smart chemical equilibrium algorithm promotes substantial savings in computational costs, resulting in comparable costs to that of transport.

to calculate the equilibrium states of all mesh cells in a time step. For the transport calculations, it is the CPU time taken to solve the algebraic transport equations (see Appendix B). Figure 5 shows that the cost for full, conventional chemical equilibrium calculations is about two orders of magnitude greater than the cost for transport calculations. It also shows that the computational cost for the machine learning algorithm, for smart equilibrium calculations, is greater than that of transport calculations *at the beginning*, but less than that for conventional Newton-based equilibrium calculations. After the initial on-demand training phase of the machine-learning-accelerated chemical equilibrium algorithm, it can be seen in Figure 5 that its computational cost stabilizes and remains below the cost of transport calculations. To note, typically, full chemical equilibrium calculations require by far the most computing time during reactive transport simulations, as also seen in Figure 5 and as stated in the introduction.

Figure 6 compares the *cumulative computational costs* of conventional and machine-learning-accelerated chemical equilibrium calculations with the cost of transport calculations. After several time steps (about 200 or at about 2000 minutes of simulated time in the figure), the cumulative computational costs for all these calculations increase at a more or less constant rate. However, it can be seen that the increment rate of the cumulative costs for the conventional equilibrium calculations, using a Newton-based method, is considerably higher than that for transport (about 45 times higher) and than that for smart, machine-learning-accelerated equilibrium calculations (about 63 times higher).

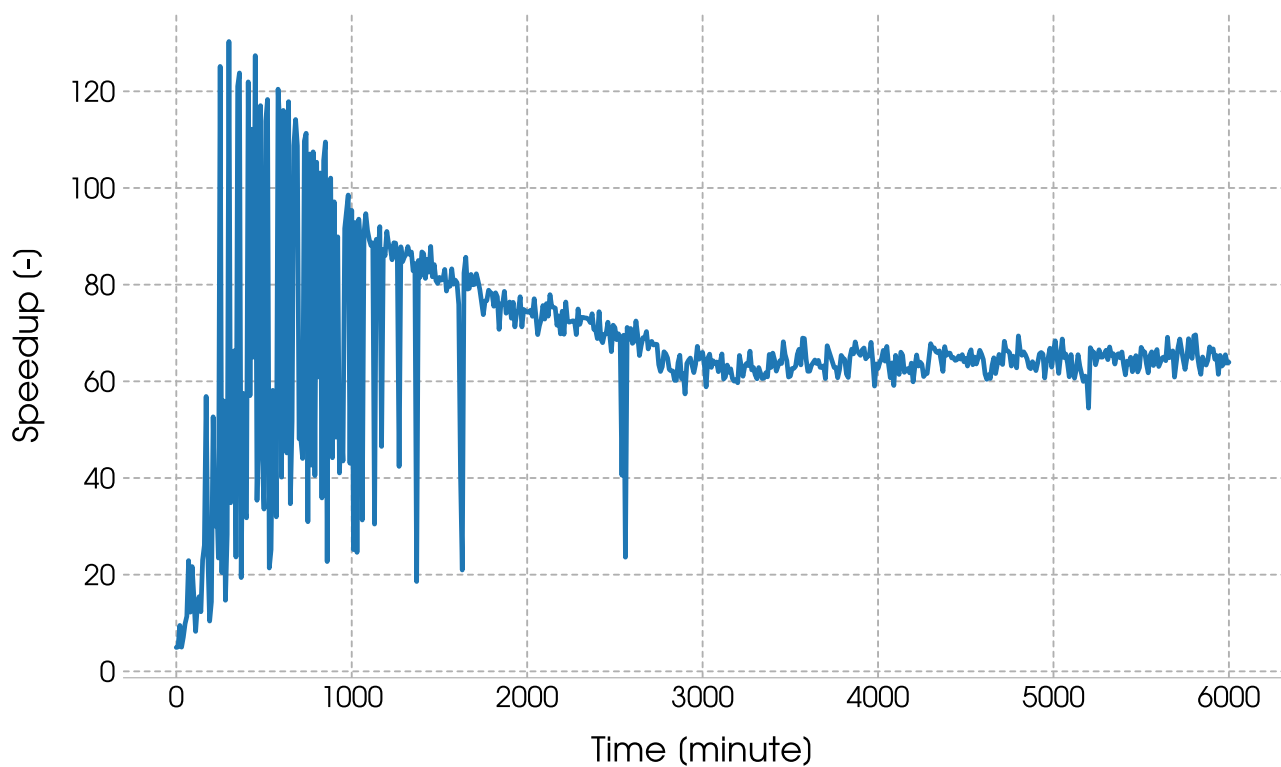


Figure 7: The speedup of chemical equilibrium calculations, at each time step of the simulation, when employing our proposed machine learning acceleration strategy for fast and accurate predictions of chemical equilibrium states. The speedup, in a time step, is calculated as the ratio of the time needed for the conventional chemical equilibrium algorithm and the time needed for the smart chemical equilibrium algorithm. **Remark:** By implementing more optimized lookup algorithms, when finding the most similar previously solved equilibrium problem (e.g., using kd-trees, which permits a search algorithm with complexity of $O(\log n)$, instead of the naive search of complexity $O(n)$ used here, where n is the number of saved equilibrium inputs), the speedup shown here will likely increase significantly.

Figure 7 shows the speedup during chemical equilibrium calculations, at each time step of the simulation, promoted by the use of the smart chemical equilibrium algorithm. The speedup at a given time step is calculated as the ratio of the CPU time needed for conventional equilibrium calculations and the CPU time for smart equilibrium calculations, performed in all mesh cells at that time step. At the beginning, during a more active on-demand training phase by the smart chemical equilibrium solver, the speedup oscillates, achieving a maximum of about 125. The oscillation is a combination of many factors, such as the need to occasionally perform full equilibrium calculations for learning purposes and the fact that the strongest compositional changes occur during the first time steps when the injected fluid perturbs its initial equilibrium. As the machine learning chemical equilibrium algorithm continues to learn how to solve different equilibrium problems, it gets to a stage that is able to quickly predict all new equilibrium states. When this happens, the speedup stabilizes at about 63 (or $10^{1.8}$), as shown in Figure 7, at later time steps.

We remark that this speedup is strongly dependent on how fast we can search for the previous equilibrium problem, closest to the one being solved. Currently, we are using a naive approach, during which all past equilibrium inputs, $\mathcal{I} = \{(T^k, P^k, b^k)\}_{k=1}^K$, are saved in a linked list data structure. This data structure is not optimal for *nearest-neighbor search algorithms*, a common procedure in computer science, such as in machine learning and computer graphics applications, because it requires each previous input (T^k, P^k, b^k) to be compared against the new equilibrium input (T^q, P^q, b^q) . As a result, this particular search algorithm has complexity $O(K)$, where K is the number of saved inputs. A more suitable data structure is a *kd-tree*, which would split the input space into several orthogonal partitions, permitting a search algorithm that succeeds, on average, after about $\log_2(K)$ comparisons. For example, instead of 256 comparisons using a linked list, we would need only $8 = \log_2(256)$ with a balanced kd-tree. Future optimization of our machine learning equilibrium method will make use of kd-trees or other fast search algorithms.

5 Conclusions and Future Work

We present a straightforward, smart, machine-learning chemical equilibrium algorithm that calculates equilibrium states in reactive transport simulations 60–125 times faster than a conventional Newton-based algorithm. The reason for this speedup is that the smart equilibrium algorithm employs a new concept of an unconventional, supervised machine learning method, with an on-demand training strategy, rather than the more common training-in-advance approach. Our new algorithm is capable of “remembering” past equilibrium calculations and performing rapid predictions of new equilibrium states, whenever the new equilibrium problem is sufficiently close to some previously solved one. These machine-learning-accelerated chemical equilibrium calculations are able to dramatically speedup reactive transport simulations, in which chemical reaction calculations are otherwise typically responsible for over 90% of all computation costs.

Our proposed machine learning algorithm differs from previous machine learning strategies to speedup chemical equilibrium calculations, because here, learning is carried out on-demand, i.e., during the actual simulation, rather than during an initial, time-consuming training phase. Consequently, our method requires no a priori insights of possible chemical conditions that may occur during the actual simulation, a problem inherent to standard, i.e., statistics-based, machine learning algorithms. These initial training sessions of standard machine learning algorithms require large data-sets of input-output information, which are sometimes randomly obtained. Furthermore, there are no clear criteria for determining when such training sessions are sufficient and can be terminated to begin with the actual simulation of interest. Finally, traditional,

statistically-based machine learning algorithms applied to chemical equilibrium calculations neither understand the thermodynamic behavior of stable phases in chemical systems nor can they straightforwardly predict chemical equilibrium states that satisfy given mass conservation constraints.

The presented smart equilibrium algorithm contains only three steps, which are computationally relatively cheap to perform. The first step performs a lookup of past equilibrium problems that are closest to the new one. The second step is a simple algebraic calculation to estimate the new equilibrium state from the previous one, more specifically, two vector additions (of dimension $N \times 1$) and a matrix-vector multiplication (the matrix with dimension $N \times E$, the vector with dimension $E \times 1$), where N and E are the number of species and elements, respectively. The third step is to check the acceptance criterion, which is also a relatively cheap compute operation. Hence, the smart approximation is able to quickly bypass extremely expensive operations, when solving chemical equilibrium problems, such as (i) the evaluation of thermodynamic properties of all species (e.g., activities) and (ii) the solution of systems of linear equations.

Since equilibrium calculations are carried out iteratively, these computationally expensive operations are performed once each iteration and, thus, several times. Even if convergence could always be established in only one iteration, this would still not cause a substantial improvement in the performance of reactive transport simulations, given the high cost of those operations. In contrast, the proposed smart equilibrium algorithm *skips all these iterations*, and their intrinsic expensive operations, and is instead able to immediately predict an accurate equilibrium state for similar problems. The new algorithm, thus, has the potential to substantially accelerate reactive transport simulations, as, indeed, demonstrated for the modeling problem in Section 4.

Potential future work and improvements of our machine learning algorithm for rapid chemical equilibrium calculations could include:

- the use of kd-trees for faster lookup operations;
- the investigation of the smart chemical equilibrium algorithm for more complex chemical systems in more heterogeneous and complex reactive transport problems per time step;
- the use of alternative acceptance criteria to further avoid unnecessary on-demand training operations;
- the use of GPUs for massively parallel smart predictions of thousands to millions of equilibrium states;
- the extension of the machine learning strategy, presented here, to chemical kinetics calculations and other problems in science and engineering;
- the application of *garbage collector ideas*, used in programming languages, such as Python and Java, to eliminate all previously saved equilibrium states that have not been used for some time;
- the implementation of strategies that rely not only on the nearest previous saved equilibrium state, but up to a certain number (e.g., the two or three closest equilibrium problems solved previously) to possibly avoid the triggering of on-demand training operations and also to improve accuracy by combining the sensitivity derivatives in different nearby states;
- incorporate spatial and temporal information in the machine learning algorithm and test if the computation cost of search operations can be decreased with it.

The above roadmap of future investigations shows how much a new machine learning algorithm for rapid chemical reaction calculations can yet be improved in addition to what we have already shown here. We believe that the use of machine-learning-accelerated algorithms for chemical reaction calculations is crucial for a significant acceleration of complex reactive transport simulations, and it is essential for a substantial decrease of the overall computational costs of chemical calculations, which so far have been responsible for 90–99% of all computing costs in large-scale numerical simulations with intricate chemistry representation.

References

- [1] Ramshaw, J. D. (1980). Partial Chemical Equilibrium in Fluid Dynamics. *Physics of Fluids*, 23(4):675–680.
- [2] Ramshaw, J. D. and Cloutman, L. D. (1981). Numerical method for partial equilibrium flow. *Journal of Computational Physics*, 39(2):405–417.
- [3] Ramshaw, J. D. and Amsden, A. A. (1985). Improved iteration scheme for partial equilibrium flow. *Journal of Computational Physics*, 59(3):484–489.
- [4] Ramshaw, J. and Chang, C. (1995). Iteration Scheme for Implicit Calculations of Kinetic and Equilibrium Chemical Reactions in Fluid Dynamics. *Journal of Computational Physics*, 116(2):359–364.
- [5] Lichtner, P. C. (1985). Continuum model for simultaneous chemical reactions and mass transport in hydrothermal systems. *Geochimica et Cosmochimica Acta*, 49(3):779–800.
- [6] Steefel, C. I. and Lasaga, A. C. (1994). A coupled model for transport of multiple chemical species and kinetic precipitation/dissolution reactions with applications to reactive flow in single phase hydrothermal systems. *American Journal of Science*, 294(5):529–592.
- [7] Steefel, C. I. and MacQuarrie, K. T. B. (1996). Approaches to modeling of reactive transport in porous media. *Reviews in Mineralogy and Geochemistry*, 34(1):83–129.
- [8] Leal, A. M., Kulik, D. A., and Saar, M. O. (2017). Ultra-Fast Reactive Transport Simulations When Chemical Reactions Meet Machine Learning: Chemical Kinetics.
- [9] Pitzer, K. S. (1973). Thermodynamics of electrolytes. I. Theoretical basis and general equations. *The Journal of Physical Chemistry*, 77(2):268–277.
- [10] Peng, D.-Y. and Robinson, D. B. (1976). A New Two-Constant Equation of State. *Industrial & Engineering Chemistry Fundamentals*, 15(1):59–64.
- [11] Leal, A. M. M., Kulik, D. A., Smith, W. R., and Saar, M. O. (2017). An overview of computational methods for chemical equilibrium and kinetic calculations for geochemical and reactive transport modeling. *Pure and Applied Chemistry*, 89(5):597–643.
- [12] White, W. B., Johnson, S. M., and Dantzig, G. B. (1958). Chemical Equilibrium in Complex Mixtures. *J. Chem. Phys.*, 28:751.

- [13] Smith, W. R. (1980). The Computation of Chemical Equilibria in Complex Systems. *Industrial & Engineering Chemistry Fundamentals*, 19(1):1–10.
- [14] Smith, W. and Missen, R. (1982). *Chemical reaction equilibrium analysis: theory and algorithms*. Wiley-Interscience, New York.
- [15] Alberty, R. A. (1992). Equilibrium calculations on systems of biochemical reactions at specified pH and pMg. *Biophysical Chemistry*, 42(2):117–131.
- [16] Crerar, D. A. (1975). A method for computing multicomponent chemical equilibria based on equilibrium constants. *Geochimica et Cosmochimica Acta*, 39(10):1375–1384.
- [17] de Capitani, C. and Brown, T. H. (1987). The computation of chemical equilibrium in complex systems containing non-ideal solutions. *Geochimica et Cosmochimica Acta*, 51(10):2639–2652.
- [18] Eriksson, G. and Thompson, W. (1989). A procedure to estimate equilibrium concentrations in multicomponent systems and related applications. *Calphad*, 13(4):389–400.
- [19] Ghiorso, M. S. (1994). Algorithms for the estimation of phase stability in heterogeneous thermodynamic systems. *Geochimica et Cosmochimica Acta*, 58(24):5489–5501.
- [20] McBride, B. J. and Gordon, S. (1971). Computer program for calculation of complex chemical equilibrium compositions rocket performance incident and reflected shocks, and Chapman-Jouguet detonations. Technical report, NASA.
- [21] McBride, B. J. and Gordon, S. (1994). Computer Program for Calculation of Complex Chemical Equilibrium Compositions and Applications: I. Analysis. Technical report.
- [22] McBride, B. J. and Gordon, S. (1996). Computer Program for Calculation of Complex Chemical Equilibrium Compositions and Applications: II-User Manual and Program Description. Technical report, NASA.
- [23] Harvey, J. P., Eriksson, G., Orban, D., and Chartrand, P. (2013). Global minimization of the gibbs energy of multicomponent systems involving the presence of order/disorder phase transitions. *American Journal of Science*, 313(3):199–241.
- [24] Harvie, C. E., Greenberg, J. P., and Weare, J. H. (1987). A chemical equilibrium algorithm for highly non-ideal multiphase systems: Free energy minimization. *Geochimica et Cosmochimica Acta*, 51(5):1045–1057.
- [25] Karpov, I. K., Chudnenko, K. V., and Kulik, D. A. (1997). Modeling chemical mass transfer in geochemical processes: Thermodynamic relations, conditions of equilibria, and numerical algorithms. *American Journal of Science*, 297(8):767–806.
- [26] Karpov, I. K., Chudnenko, K. V., Kulik, D. A., Avchenko, O. V., and Bychinski, V. A. (2001). Minimization of Gibbs free energy in geochemical systems by convex programming. *Geochemistry International*, 39(11):1108–1119.
- [27] Karpov, I. K., Chudnenko, K. V., Kulik, D. A., and Bychinskii, V. A. (2002). The convex programming minimization of five thermodynamic potentials other than Gibbs energy in geochemical modeling. *American Journal of Science*, 302(4):281–311.

- [28] Koukkari, P. and Pajarre, R. (2011). A Gibbs energy minimization method for constrained and partial equilibria. *Pure and Applied Chemistry*, 83(6):1243–1254.
- [29] Kulik, D. A., Wagner, T., Dmytrieva, S. V., Kosakowski, G., Hingerl, F. F., Chudnenko, K. V., and Berner, U. R. (2013). GEM-Selektor geochemical modeling package: revised algorithm and GEMS3K numerical kernel for coupled simulation codes. *Computational Geosciences*, 17(1):1–24.
- [30] Leal, A. M. M., Blunt, M. J., and LaForce, T. C. (2013). A robust and efficient numerical method for multiphase equilibrium calculations: Application to CO₂-brine-rock systems at high temperatures, pressures and salinities. *Advances in Water Resources*, 62(Part C):409–430.
- [31] Leal, A. M., Blunt, M. J., and LaForce, T. C. (2014). Efficient chemical equilibrium calculations for geochemical speciation and reactive transport modelling. *Geochimica et Cosmochimica Acta*, 131:301–322.
- [32] Leal, A. M., Kulik, D. A., and Kosakowski, G. (2016a). Computational methods for reactive transport modeling: A Gibbs energy minimization approach for multiphase equilibrium calculations. *Advances in Water Resources*, 88:231–240.
- [33] Leal, A. M., Kulik, D. A., Kosakowski, G., and Saar, M. O. (2016b). Computational methods for reactive transport modeling: An extended law of mass-action, xLMA, method for multiphase equilibrium calculations. *Advances in Water Resources*, 96:405–422.
- [34] Morel, F. and Morgan, J. (1972). Numerical method for computing equilibria in aqueous chemical systems. *Environmental Science & Technology*, 6(1):58–67.
- [35] Néron, A., Lantagne, G., and Marcos, B. (2012). Computation of complex and constrained equilibria by minimization of the Gibbs free energy. *Chemical Engineering Science*, 82:260–271.
- [36] Nordstrom, D., Plummer, L. N., Wigley, T., Wolery, T., Ball, J., Jenne, E., Bassett, R., Crerar, D., Florence, T., Fritz, B., Hoffman, M., Holdren, G., Jr., L. G., Mattigod, S., McDuff, R., Morel, F., Reddy, M., and Sposito, G. (1979). A comparison of computerized chemical models for equilibrium calculations in aqueous systems. *American Chemical Society Symposium Series*, 93:857–892.
- [37] Trangenstein, J. A. (1987). Customized minimization techniques for phase equilibrium computations in reservoir simulation. *Chemical Engineering Science*, 42(12):2847–2863.
- [38] van Zeggeren, F. and Storey, S. H. (1970). *The Computation of Chemical Equilibria*. Cambridge University Press, London, England.
- [39] Voňka, P. and Leitner, J. (1995). Calculation of chemical equilibria in heterogeneous multi-component systems. *Calphad*, 19(1):25–36.
- [40] Wolery, T. J. and Walters, L. J. (1975). Calculation of equilibrium distributions of chemical species in aqueous solutions by means of monotone sequences. *Journal of the International Association for Mathematical Geology*, 7(2):99–115.
- [41] Zeleznik, F. J. and Gordon, S. (1960). An analytical investigation of the general methods of calculating chemical equilibrium compositions. (NASA-TN-D-473).

- [42] Jatnieks, J., De Lucia, M., Dransch, D., and Sips, M. (2016). Data-driven Surrogate Model Approach for Improving the Performance of Reactive Transport Simulations. *Energy Procedia*, 97:447–453.
- [43] Parkhurst, D. and Appelo, C. (2013). Description of input and examples for PHREEQC version 3—A computer program for speciation, batch-reaction, one-dimensional transport, and inverse geochemical calculations. In *Groundwater Book 6, Modeling Techniques*, chapter A43, page 497. U.S. Geological Survey Techniques and Methods.
- [44] Leal, A. M., Kulik, D. A., and Saar, M. O. (2016). Enabling Gibbs energy minimization algorithms to use equilibrium constants of reactions in multiphase equilibrium calculations. *Chemical Geology*, 437:170–181.
- [45] Helgeson, H. C. and Kirkham, D. H. (1974a). Theoretical prediction of the thermodynamic behavior of aqueous electrolytes at high pressures and temperatures: I. Summary of the thermodynamic/electrostatic properties of the solvent. *American Journal of Science*, 274(10):1089–1198.
- [46] Helgeson, H. C. and Kirkham, D. H. (1974b). Theoretical prediction of the thermodynamic behavior of aqueous electrolytes at high pressures and temperatures: II. Debye-Huckel parameters for activity coefficients and relative partial molal properties. *American Journal of Science*, 274(10):1199–1261.
- [47] Helgeson, H. C. and Kirkham, D. H. (1976). Theoretical prediction of the thermodynamic properties of aqueous electrolytes at high pressures and temperatures: III. Equation of state for aqueous species at infinite dilution. *American Journal of Science*, 276(2):97–240.
- [48] Helgeson, H. C., Kirkham, D. H., and Flowers, G. C. (1981). Theoretical prediction of the thermodynamic behavior of aqueous electrolytes at high pressures and temperatures: IV. Calculation of activity coefficients, osmotic coefficients, and apparent molal and standard and relative partial molal properties to 600 C. *American Journal of Science*, 281(10):1249–1516.
- [49] Drummond, S. (1981). *Boiling and mixing of hydrothermal fluids: chemical effects on mineral precipitation*. Ph.d., Pennsylvania State University.
- [50] Helgeson, H. C., Delany, J. M., Nesbitt, H. W., and Bird, D. K. (1978). Summary and critique of the thermodynamic properties of rock-forming minerals. *American Journal of Science*, 278 A(1):229.
- [51] Tanger, J. C. and Helgeson, H. C. (1988). Calculation of the thermodynamic and transport properties of aqueous species at high pressures and temperatures; revised equations of state for the standard partial molal properties of ions and electrolytes. *American Journal of Science*, 288(1):19–98.
- [52] Shock, E. and Helgeson, H. C. (1988). Calculation of the thermodynamic and transport properties of aqueous species at high pressures and temperatures: Correlation algorithms for ionic species and equation of state predictions to 5 kb and 1000°C. *Geochimica et Cosmochimica Acta*, 52(8):2009–2036.

- [53] Shock, E. L., Oelkers, E. H., Johnson, J. W., Sverjensky, D. A., and Helgeson, H. C. (1992). Calculation of the thermodynamic properties of aqueous species at high pressures and temperatures. Effective electrostatic radii, dissociation constants and standard partial molal properties to 1000 °C and 5 kbar. *Journal of the Chemical Society, Faraday Transactions*, 88(6):803.
- [54] Johnson, J. W., Oelkers, E. H., and Helgeson, H. C. (1992). SUPCRT92: A software package for calculating the standard molal thermodynamic properties of minerals, gases, aqueous species, and reactions from 1 to 5000 bar and 0 to 1000 C. *Computers & Geosciences*, 18(7):899–947.
- [55] Wagner, W. and Pruss, A. (2002). The IAPWS Formulation 1995 for the Thermodynamic Properties of Ordinary Water Substance for General and Scientific Use. *Journal of Physical and Chemical Reference Data*, 31(2):387.
- [56] Nocedal, J. and Wright, S. J. (1999). *Numerical Optimization*. Springer, 2nd edition.
- [57] Fletcher, R. (2000). *Practical Methods of Optimization*. Wiley, 2nd edition.

A Chemical Equilibrium Equations

The solution of the Gibbs energy minimization problem in equation (4) needs to satisfy the following *Karush–Kuhn–Tucker (KKT) conditions*, or *first-order optimality conditions*, for a local minimum of the Gibbs energy function G [56, 57]:

$$\mu - A^T y - z = 0, \quad (16)$$

$$An - b = 0, \quad (17)$$

$$n_i z_i = 0 \quad (i = 1, \dots, N), \quad (18)$$

$$n_i \geq 0 \quad (i = 1, \dots, N), \quad (19)$$

$$z_i \geq 0 \quad (i = 1, \dots, N), \quad (20)$$

where $y = (y_1, \dots, y_E)$ and $z = (z_1, \dots, z_N)$ are introduced *Lagrange multipliers* that need to be solved along with the species amounts $n = (n_1, \dots, n_N)$. For more details about these Lagrange multipliers and their interpretation as well as instructions on how to efficiently solve these equations, see Leal et al. [11, 32].

The previous chemical equilibrium equations can be written in an *extended law of mass action (xLMA)* formulation as:

$$\ln K - v(\ln a + \ln w) = 0, \quad (21)$$

$$An - b = 0, \quad (22)$$

$$n_i \ln w_i = 0 \quad (i = 1, \dots, N), \quad (23)$$

$$n_i \geq 0 \quad (i = 1, \dots, N), \quad (24)$$

$$0 < w_i \leq 1 \quad (i = 1, \dots, N) \quad (25)$$

following the use of the extended law of mass action equations:

$$K_m = \prod_{i=1}^N (a_i w_i)^{v_{mi}} \quad (26)$$

associated with the M linearly independent chemical reactions among the N chemical species in equilibrium:

$$0 \rightleftharpoons \sum_{i=1}^N v_{mi} \alpha_i \quad (m = 1, \dots, M), \quad (27)$$

where $K = (K_1, \dots, K_M)$ is the vector of *equilibrium constants* of the reactions, with $K_m = K_m(T, P)$ denoting the equilibrium constant of the m th reaction, and v the $M \times N$ *stoichiometric matrix* of these chemical reactions, with v_{mi} denoting the stoichiometric coefficient of the i th species in the m th reaction with the convention that v_{mi} is positive if the i th species is a product in the m th reaction, and negative if a reactant. Moreover, $w = (w_1, \dots, w_N)$ is the vector of *species stability factors* that need to be solved along with the species amounts $n = (n_1, \dots, n_N)$. These factors are introduced to ensure that the extended law of mass action equations (26) are valid even when some species in their corresponding reactions are unstable at equilibrium (i.e., when a species belongs to a phase that is absent from equilibrium). When all species are stable at equilibrium, it follows that $w_i = 1$ and the xLMA equations reduce to the conventional LMA equations:

$$K_m = \prod_{i=1}^N \alpha_i^{v_{mi}}. \quad (28)$$

The number of linearly independent chemical reactions among the N species in equilibrium is $M = N - C$, where $C = \text{rank}(A)$, and thus whenever the formula matrix A is full rank, $C = E$ and $M = N - E$. For more information on how to solve these equations and how they are related to the conventional law of mass action equations, see Leal et al. [11, 33].

B Reactive Transport Equations

The fundamental mass conservation equations for both fluid and solid species are:

$$\frac{\partial n_i^f}{\partial t} + \nabla \cdot (\mathbf{v} n_i^f - D \nabla n_i^f) = r_i^f \quad (i = 1, \dots, N^f), \quad (29)$$

$$\frac{\partial n_i^s}{\partial t} = r_i^s \quad (i = 1, \dots, N^s), \quad (30)$$

where n_i^f and n_i^s are the *bulk concentration* of the i th fluid and solid species (in mol/m³), respectively; \mathbf{v} is the fluid pore velocity (in m/s); D is the diffusion coefficient of the fluid species (in m²/s); r_i^f and r_i^s are the rates of production/consumption of the i th fluid and solid species (in mol/s), respectively, due to chemical reactions; and N^f and N^s are the number of fluid and solid species, respectively. Note that the above equations assume a single fluid phase and common diffusion coefficients for all fluid species.

By partitioning the species as fluid and solid species, the formula matrix, A , can be conveniently represented as:

$$A = [A^f \quad A^s], \quad (31)$$

where A^f and A^s are the formula matrices of the fluid and solid partitions (i.e., the matrices constructed from the columns of A corresponding to fluid and solid species). The concentrations of elements in both fluid and solid partitions, b_j^f and b_j^s , can then be calculated from the species concentrations in the same partition using:

$$b_j^f = \sum_{i=1}^{N^f} A_{ji}^f n_i^f \quad (j = 1, \dots, E) \quad (32)$$

and

$$b_j^s = \sum_{i=1}^{N^s} A_{ji}^s n_i^s \quad (j = 1, \dots, E). \quad (33)$$

Recall that the rates of production of the species, r_i^f and r_i^s , are exclusively due to chemical reactions. Let r_i denote the rate of production/consumption of the i th species in the system, and not in a fluid/solid partition. From the mass conservation condition for the elements (chemical elements and electrical charge), it follows that:

$$\underbrace{\sum_{i=1}^N A_{ji} r_i}_{\text{rate of production of element } j} = \underbrace{\sum_{i=1}^{N^f} A_{ji}^f r_i^f}_{\text{rate of production of element } j \text{ in the fluid partition}} + \underbrace{\sum_{i=1}^{N^s} A_{ji}^s r_i^s}_{\text{rate of production of element } j \text{ in the solid partition}} = 0, \quad (34)$$

which is the mathematical statement for the fact that *elements are neither created nor destroyed* during chemical reactions. We can combine this result with equations (29) and (30) to derive the following conservation equations for the elements:

$$\frac{\partial b_j^s}{\partial t} + \frac{\partial b_j^f}{\partial t} + \nabla \cdot (\mathbf{v} b_j^f - D \nabla b_j^f) = 0 \quad (j = 1, \dots, E). \quad (35)$$

Assume that all species, fluid and solid, are in *local chemical equilibrium everywhere, at all times*. One can then perform *operator splitting steps* to solve the fundamental mass conservation equations (29) and (30) to calculate the concentrations of the species, n_i , over time. Let k denote the current *time step* and Δt the *time step length* used in the discretization of the time derivative terms. The operator splitting steps at the k th time step are:

Step 1) update the concentrations of the elements in the fluid partition using:

$$\frac{\tilde{b}_j^{f,k+1} - b_j^{f,k}}{\Delta t} + \nabla \cdot (\mathbf{v} \tilde{b}_j^{f,k+1} - D \nabla \tilde{b}_j^{f,k+1}) = 0 \quad (j = 1, \dots, E),$$

where $\tilde{b}_j^{f,k}$ is the known concentration of the j th element at time step k in the fluid partition and $\tilde{b}_j^{f,k+1}$ is its unknown concentration at the next time step. Note that an implicit scheme is assumed for both advection and diffusion rates.

Step 2) update the total concentrations of the elements:

$$b_j^{k+1} = \tilde{b}_j^{f,k+1} + b_j^{s,k}. \quad (36)$$

Step 3) calculate the concentrations of the species, n_i^{k+1} , in each mesh cell, using a conventional or the proposed smart chemical equilibrium algorithm. For this, use the local temperature and pressure values together with the *updated local concentrations of elements*, b_j^{k+1} as inputs.